Arene−Mercury Complexes Stabilized Aluminum and Gallium Chloride: Synthesis and Structural Characterization

Alexander S. Borovik,[1a] Simon G. Bott,[1b] and Andrew R. Barron*,[1a]

Contribution from the Department of Chemistry and Center for Nanoscale Science and Technology, Rice University, Houston, Texas 77005, and Department of Chemistry, University of Houston, Houston, Texas 77204

Received April 20, 2001

Abstract: Reaction of $HgCl_2$ with 2 equiv of MCl_3 in an aromatic solvent yields $Hg(arene)_2(MCl_4)_2$ where, arene = C_6H_5Me, M = Al (**1**), Ga (**2**); arene = C_6H_5Et, M = Al (**3**) and Ga (**4**); *o*-$C_6H_4Me_2$, M = Al (**5**), Ga (**6**); C_6H_3-1,2,3-Me_3, M = Al (**7**) and Ga (**8**). The solid-state structures of compounds **1**−**5** and **7** have been determined by X-ray crystallography. In the solid state, compounds **1**−**4** and **7** exist as neutral complexes in which two arenes are bound to the mercury, and the MCl_3 groups are bound through bridging chlorides to the mercury; compound **5** exists as a cation−anion pair $[Hg(o\text{-}C_6H_4Me_2)_2(AlCl_4)][AlCl_4]$. However, in solution compounds **1**−**8** all exist as neutral complexes. The structures of $Hg(arene)_2(AlCl_4)_2$ and $[Hg(arene)_2(AlCl_4)]^+$ have been determined by DFT calculations {B3LYP level} to facilitate the assignment of the ^{13}C CPMAS NMR spectra and are in good agreement with the X-ray diffraction structures of compounds **1** and **5**. Reaction of $HgCl_2$ with MCl_3 in benzene, *m*-xylene, and *p*-xylene results in the formation of liquid clathrates whose spectroscopic characterization is consistent with ionic structures, $[Hg(arene)_2(MCl_4)][MCl_4]$. The calculated energy difference between $Hg(C_6H_5Me)_2(AlCl_4)_2$ and $[Hg(C_6H_5Me)_2(AlCl_4)][AlCl_4]$ is discussed with respect to the structure of compound **5** in the solid state versus solution state and the proposed speciation in the liquid clathrates.

Introduction

Group 13 halides are well-known as catalysts for the Friedel−Crafts alkylation and acylation of aromatic hydrocarbons. The highly Lewis acidic group 13 halide activates the alkyl or acyl halide, via either complexation or ionization (e.g., eq 1),[2] by placing a positive charge on the β-substituent (Figure 1a).

$$RCl + AlCl_3 \rightleftharpoons RCl\cdots AlCl_3 \rightleftharpoons [R]^+[AlCl_4]^- \qquad (1)$$

The increase of positive charge on the β-substituent is a general effect of the coordination of aluminum Lewis acids to both organic (Figure 1b) and inorganic (Figure 1c) carbonyls, for example, activation of ketones to alkylation and reduction[3] and activation of transition metal carbonyl ligands toward the methyl migration.[4] We have recently observed that the coordination of an alcohol to an aluminum Lewis acid results in an increase of the pK_a of the alcohol O−H by at least 7 units.[5] Although seemingly unrelated, this activation may also be considered as an example of placing an increased positive charge on the β-substituent, the alcohol hydrogen (Figure 1d), hence increasing its electrophilicity and making it more susceptible to reaction with nucleophiles such as aluminum alkyls.

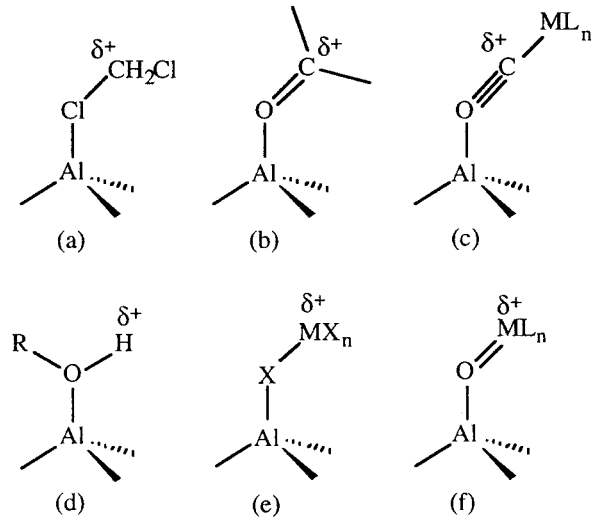

Figure 1. Schematic representation of the "activation" of organic and inorganic substrates by aluminum Lewis acids.

There has been an increased interest in the development of new Lewis acidic compounds as catalysts and cocatalysts, especially with regard to olefin polymerization. Most of these efforts have focused on using electron-withdrawing substituents, low coordination numbers, or multiple centers.[6] As an alternative approach, applying the concept of increasing the Lewis acidity

* To whom correspondence should be addressed. Web site: http://www.rice.edu/barron.

(1) (a) Department of Chemistry, Rice University. (b) Department of Chemistry, University of Houston.

(2) (a) Whitmore, F. C. *J. Am. Chem. Soc.* **1932**, *54*, 3274. (b) Olah, G. A.; Kuhn, S. J.; Flood, S. H. *J. Am. Chem. Soc.* **1962**, *84*, 1688. (c) Olah, G. A.; Kobayashi, S.; Tashiro, M. *J. Am. Chem. Soc.* **1972**, *94*, 7448.

(3) (a) Power, M. B.; Nash, J. R.; Healy, M. D.; Barron, A. R. *Organometallics* **1992**, *11*, 1830. (b) Power, M. B.; Bott, S. G.; Atwood, J. L.; Barron, A. R. *J. Am. Chem. Soc.* **1990**, *112*, 3446. (c) Power, M. B.; Bott, S. G.; Clark, D. L.; Atwood, J. L.; Barron, A. R. *Organometallics* **1990**, *9*, 3086 and references therein.

(4) (a) Butts, S. B.; Holt, E. M.; Strauss, S. H.; Alcock, N. W.; Stimson, R. E.; Shriver, D. F. *J. Am. Chem. Soc.* **1979**, *101*, 5864. (b) Butts, S. Beda; Strauss, S. H.; Holt, E. M.; Stimson, R. E.; Alcock, N. W.; Shriver, D. F. *J. Am. Chem. Soc.* **1980**, *102*, 5093.

(5) McMahon, C. N.; Bott, S. G.; Barron, A. R. *J. Chem. Soc., Dalton Trans.* **1997**, 3129.

10.1021/ja011003u CCC: $20.00
Published on Web 10/20/2001

Table 1. Selected Bond Lengths (Å) and Angles (deg) in $Hg(arene)_2(MCl_4)_2$

M arene	Al C_6H_5Me (**1**)	Ga C_6H_5Me (**2**)[a]	Al C_6H_5Et (**3**)	Ga C_6H_5Et (**4**)	Al *o*-$C_6H_4Me_2$ (**5**)	Al C_6H_3-1,2,3-Me_3 (**7**)
Hg−C	2.32(1)	2.349(9)	2.30(1)	2.33(1)	2.27(2), 2.40(2)	2.405(9), 2.44(1)
	2.72(1)	2.71(1)	2.72(2)	2.75(2)	2.64(2), 2.74(2)	2.45(1), 2.46(1)
Hg−Cl	2.677(2)	2.652(2)	2.648(4)	2.634(4)	2.761(3), 2.768(3)	2.661(2), 2.758(3)
M-Cl_{br}	2.176(4)	2.239(2)	2.184(5)	2.230(4)	2.166(4), 2.156(5)	2.181(4), 2.178(4)
M-Cl_{ter}	2.102(5)−2.118(3)	2.144(3)−2.166(3)	2.080(6)−2.169(5)	2.128(4)−2.155(4)	2.09(1)−2.169(5)	2.103(5)−2.124(4)
Cl−Hg−Cl	81.1(1)	82.4(1)	84.5(6)	85.6(2)	75.2(1)	89.90(8)
C−Hg−C	135.1(5)	131.3(6)	129(1)	126(1)	125.5(6)	140.0(4)
Hg−Cl-M	110.2(2)	110.6(1)	112.3(2)	111.4(2)	90.8(1), 91.2(1)	106.1(1), 107.9(1)

[a] Borovik, A. S.; Bott, S. G.; Barron, A. R. *Angew. Chem., Int. Ed.* **2000**, *39*, 4117.

of metals through their "activation" by another Lewis acid (Figure 1e) has drawn our interest. In this regard we note that aluminum halides have been previously employed as activators for transition metals through a similar complexation (see Figure 1f).[7]

Although the Lewis acid behavior of mercuracarboranes has been extensively studied by Hawthorne and co-workers,[8] the Lewis acidic nature of group 12 halides, in particular those of mercury, has been studied much less than that of the group 13 halides.[9] However, the chemistry of mercury(II) salts with aromatic hydrocarbons is well developed regarding electrophilic attack on aromatic compounds (aromatic mercuration), and Olah et al. have shown that Hg−arene complexes are involved as intermediates.[10] Kochi and co-workers have shown that the activation of the arene is related to a charge-transfer transition in the π-complex.[11,12] Crabtree and co-workers have proposed a π-complex as a key intermediate in a variety of photochemical C−C bond forming reactions,[13] while the characterization of a series of Hg(I)−arene complexes has been reported.[14] Mercury(II)−arene complexes are well-established as important intermediates, however, simple complexes have only been characterized spectroscopically.[15] The only structural characterization of a nonsolvate mercury(II) complex was reported by Kochi and co-workers with a highly electronegative trifluoroacetate ligand.[16] Based on the possibility that group 13 halide Lewis acids could "activate" other weaker Lewis acids, we have investigated the effect of $AlCl_3$ and $GaCl_3$ on the stability of Hg···arene complexes.

Results and Discussion

The reaction of $HgCl_2$ with 2 mol equiv of MCl_3 (M = Al, Ga) in a substituted aromatic solvent ($C_6H_{6-x}R_x$) yields a colored solution (yellow to orange, depending on the arene), from which crystalline material may be obtained in moderate to high yield (eq 2) for C_6H_5Me, M = Al (**1**), Ga (**2**);[17] C_6H_5Et, M = Al (**3**), Ga (**4**); *o*-$C_6H_4Me_2$, M = Al (**5**), Ga (**6**); C_6H_3-1,2,3-Me_3, M = Al (**7**), Ga (**8**).

$$HgCl_2 + MCl_3 \rightarrow Hg(arene)_2(MCl_4)_2 \qquad (2)$$

In contrast, reaction of $HgCl_2$ with 2 mol equiv of $AlCl_3$ in benzene, *m*-xylene, *p*-xylene yields liquid clathrates, see below.

Compounds **1**−**8** are stable when exposed to O_2, CO, and CO_2, but decompose upon irradiation by ambient light, exposure to moisture, or being subjected to chlorinated or coordinating solvents (e.g., $CHCl_3$, THF, Et_2O and MeCN). The solubility of each compound in its respective solvent (i.e., compound **1** in toluene) suggests a simple Lewis acid−base complex of the metal halides rather than a cation/anion pair, vide infra. This is supported by solution conductivity measurements that indicate neutral compounds in solution for compounds **1**−**8**. Although elemental analysis is consistent with the given formulas and the EI mass spectrum confirms the presence of the arene (see Experimental Section), the solution ^1H and ^{13}C NMR do not allow for structural determination due to the H/D exchange with other aromatic solvents, for example, C_6D_6.[17,18] However, the solid-state structures of compounds **1**−**5** and **7** have been determined by X-ray crystallography.

X-ray Crystallography. The molecular structures of compounds **1**, **3**, **5**, and **7** are shown in Figures 2−5, respectively. Compounds **2**[17] and **4** are isomorphous with their aluminum analogues.[19] Selected bond lengths and angles for compounds **1**−**5** and **7** are given in Table 1. The solid-state structures of $Hg(arene)_2(MCl_4)_2$ appear to fall into two general categories:

(6) See, for example: (a) Radzewich, C. E.; Guzei, I. A.; Jordan, R. F. *J. Am. Chem. Soc*. **1999**, *121*, 8673. (b) Korolev, A. V.; Guzei, I. A.; Jordan, R. F. *J. Am. Chem. Soc*. **1999**, *121*, 11606. (c) Dagorne, S.; Guzei, I. A.; Coles, M. P.; Jordan, R. F. *J. Am. Chem. Soc*. **2000**, *122*, 274. (d) Munoz-Hernandez, M.; Keizer, T. S.; Parkin, S.; Patrick, B.; Atwood, D. A. *Organometallics* **2000**, *19*, 4416. (e) Atwood, D. A.; Jegier, J. *J. Chem. Soc., Chem. Commun.* **1996**, 1507. (f) Nelson, S. G.; Kim, B.; Peelen, T. J. *J. Am. Chem. Soc*. **2000**, *122*, 9318. (g) Wuest, J. D., *Acc. Chem. Res*. **1999**, *32*, 81, and references therein.

(7) (a) Le N.; Jean P.; Youinou, M. T.; Osborn, J. A. *Organometallics* **1992**, *11*, 2413. (b) Le N.; Jean P.; Osborn, J. A. *Organometallics* **1991**, *10*, 1546.

(8) See, for example: (a) Hawthorne, M. F.; Zheng, Z. *Acc. Chem. Res*. **1997**, 30, 267. (b) Hawthorne, M. F.; Yang, X.; Zheng, Z. *Pure Appl. Chem*. **1994**, 66, 245. (c) Lee, H.; Diaz, M.; Knobler, C. B.; Hawthorne, M. F. *Angew. Chem., Int. Ed*. **2000**, *39*, 776. (d) Lee, H.; Diaz, M.; Hawthorne, M. F. *Tetrahedron Lett*. **1999**, 40, 7651. (e) Badr, I. H. A.; Diaz, M.; Hawthorne, M. F.; Bachas, L. G. *Anal. Chem*. **1999**, *71*, 1371 and references therein.

(9) (a) *The Chemistry of Mercury*; McAuliffe, C. A., Ed.; Macmillan: Toronto, 1977. (b) Dean, P. A. W. *Prog. Inorg. Chem*. **1978**, 24, 109. (c) Tschinkl, M.; Schier, A.; Riede, J.; Gabbaï, F. P. *Organometallics* **1999**, *18*, 2040. (d) Saito, S.; Zhang, J.; Koizumi, T. *J. Org. Chem*. **1998**, 63, 6029. (e) Zhuang, R.; Mueller, A. H. E. *Macromolecules* **1995**, *28*, 8043. (f) Persson, I.; Sandstroem, M.; Goggin, P. L. *Inorg. Chim. Acta* **1987**, 129, 183. (g) Wuest, J. D.; Zacharie, B. *Organometallics* **1985**, *4*, 410 and references therein.

(10) See, for example: Olah, G. A.; Yu, S. H.; Parker, D. G. *J. Org. Chem*. **1976**, *41*, 1983 and references therein.

(11) Lau, W.; Kochi, J. K. *J. Am. Chem. Soc*. **1986**, *108*, 6720.

(12) Fukuzumi, S.; Kochi, J. K. *J. Org. Chem*. **1981**, *46*, 4116.

(13) Fowley, L. A.; Less, J. C., Jr.; Crabtree, R. H.; Siegbahn, P. E. M. *J. Organomet. Chem*. **1995**, *505*, 57.

(14) Frank, W.; Dincher, B., *Z. Naturforsch*. **1987**, *42b*, 828.

(15) (a) Damude, L. C.; Dean, P. A. W. *J. Organomet. Chem*. **1979**, *181*, 1. (b) Damude, L. C.; Dean, P. A. W.; Sefcik, M. D.; Schaefer, J. *J. Organomet. Chem*. **1982**, *226*, 105.

(16) W. Lau, J. C. Huffman, and J. K. Kochi, *J. Am. Chem. Soc*. **1982**, *104*, 5515.

(17) We have previously reported the isolation and structural characterization of $[Hg(C_6H_5Me)_2(GaCl_4)_2]$: Borovik, A. S.; Bott, S. G.; Barron, A. R. *Angew. Chem., Int. Ed.* **2000**, *39*, 4117.

(18) Borovik, A. S.; Bott, S. G.; Barron, A. R. ACS National Meeting, American Chemical Society: Washington, DC, August, 2000.

(19) Although the molecular structures of compounds **6** and **8** have not been determined by X-ray crystallography due to twinning issues, the observation of a "double cell" as compared to their aluminum analogues (along with their spectroscopic characterization) suggests that compounds **6** and **8** are isostructural to compounds **5** and **7**, respectively.

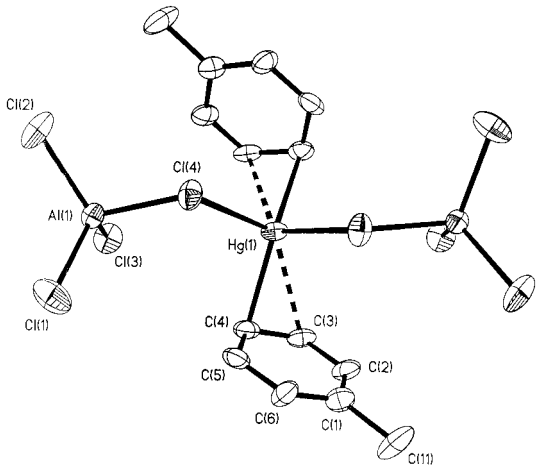

Figure 2. Molecular structure of $Hg(C_6H_5Me)_2(AlCl_4)_2$ (**1**). Thermal ellipsoids shown at the 30% level, and hydrogen atoms are omitted for clarity.

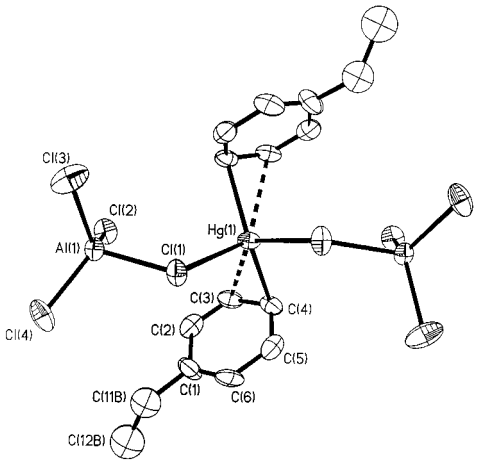

Figure 3. Molecular structure of $Hg(C_6H_5Et)_2(AlCl_4)_2$ (**3**). Thermal ellipsoids shown at the 20% level, and hydrogen atoms are omitted for clarity.

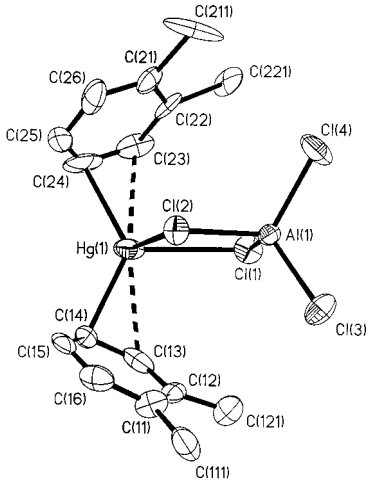

Figure 4. Molecular structure of the $[Hg(C_6H_4Me_2)_2(AlCl_4)]$ cation (**5**). Thermal ellipsoids shown at the 30% level, and hydrogen atoms are omitted for clarity.

neutral (C_6H_5Me, C_6H_5Et, and C_6H_3-1,2,3-Me_3) and ionic (*o*-$C_6H_4Me_2$). Irrespective of the overall charge of the mercury complex, the two arene ligands are π-bound to the mercury center (see Figures 2−5). The substituted arene ligands are oriented in a *rac* manner in compounds **1**−**4** and **7** (cf., Figures 2, 3, and 5). In contrast, the *o*-xylenes in compound **5** are in a meso orientation (see Figure 4).

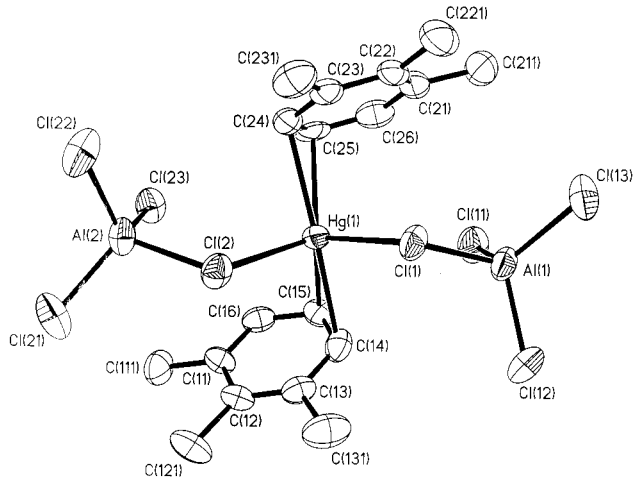

Figure 5. Molecular structure of $Hg(C_6H_3$-1,2,3-$Me_2)_2(AlCl_4)_2$ (**7**). Thermal ellipsoids shown at the 30% level, and hydrogen atoms are omitted for clarity.

As may be seen from Table 1, each arene in compounds **1**−**5** is bound in a highly asymmetric η^2 manner with the Hg−C bond para to the arene's methyl substituent being shorter (0.34−0.42 Å) than the bond in the meta position. The calculated structures for the neutral complexes, $Hg(C_6H_6)_2(AlCl_4)_2$ and $Hg(C_6H_5Me)_2(AlCl_4)_2$, and the presence of a single ^{13}C CPMAS NMR resonance, per arene ring, assignable to Hg−C for compounds **1**−**6** are consistent with η^1 rather than η^2 coordination of the arene (see below). The coordination of the two C_6H_3-1,2,3-Me_3 ligands in compound **7** appears to be closer to η^2 coordination, see Table 1. This is confirmed by ^{13}C CPMAS NMR spectroscopy, see below. It is noteworthy that the crystal structure of compound **7** is the only one of those discussed herein with arene···arene π-stacking; the intermolecular distance of 3.31 Å is less than the sum of the van der Waal radii of the arene rings (3.7 Å).[20]

It should be noted that the Hg−C distances in compounds **1**−**5** are on either side of the values reported by Kochi and co-workers for $[Hg_2(\mu\text{-}O_2CCF_3)_4(\eta^2\text{-}C_6Me_6)_2]$ (2.56 and 2.58 Å)[12] and are significantly shorter than those observed for the intramolecular Hg···arene interactions (ca. 3.2 Å).[21] Furthermore, the Hg−C distances in compounds **1**−**5** are shorter than those observed for the Hg(I)−arene complex, $[Hg_2(C_6M_6)][AlCl_4]_2$,[14] [2.43(3) and 2.41(3) Å] in which the arene is a stronger π-donor. It is also worth noting that a typical Hg−C σ-bond is 2.1−2.2 Å[22] in length which is only slightly shorter than the shortest Hg−C interactions in the compounds discussed herein, see Table 1. Although the Kochi complex was the first crystallographically characterized mercury−arene π-complex, several examples had been spectroscopically characterized,[23,24] and Tsunoda and Gabbaï have recently reported the structural characterization of a benzene "solvate" supramolecule that contains a μ^6-η^2:η^2:η^2:η^2:η^2:η^2 benzene sandwiched between six $[Hg_3(C_6F_4)_3]$ units.[25]

(20) *Handbook of Chemistry and Physics*, 60th ed.; CRC Press: Boca Raton, Florida, 1980; p D-194.
(21) (a) Lampe, P. A.; Moore, P. *Inorg. Chim. Acta* **1979**, *36*, 27. (b) Cathy, A. J.; Chaichit, N.; Gatehouse, B. M. *Acta Crystallogr., Sect. B* **1980**, *36*, 786.
(22) Kamenar, B.; Penavic, M. *Inorg. Chim. Acta* **1972**, *6*, 191.
(23) Eliezer, I.; Avinur, P. *J. Chem. Phys.* **1971**, *55*, 2300.
(24) Vezzosi, I. M.; Peyronel, G.; Zanoli, A. F. *Inorg. Chim. Acta* **1974**, *8*, 229.
(25) Tsunoda, M.; Gabbaï, F. P. *J. Am. Chem. Soc.* **2000**, *122*, 8335.

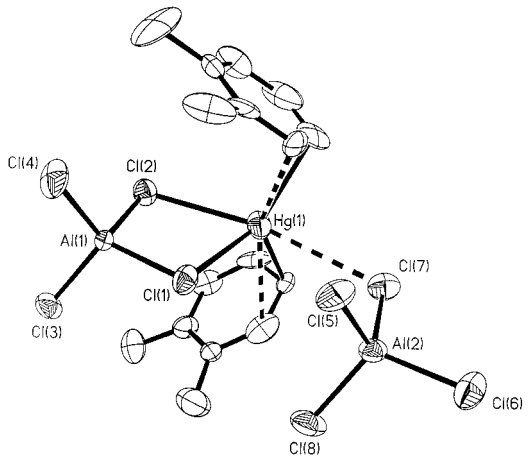

Figure 6. View of the close cation/anion interaction in $[Hg(C_6H_4Me_2)_2(AlCl_4)][AlCl_4]$. Thermal ellipsoids shown at the 30% level, and hydrogen atoms are omitted for clarity.

The X-ray structure of compound **5** shows it to be a cation/anion pair in the solid state, that is, $[Hg(C_6H_4Me_2)_2(AlCl_4)][AlCl_4]$, in which the coordinated $AlCl_4$ moiety is bound λ^2 to the mercury (Figure 4), rather than λ^1 as observed in compounds **1**−**4** and **7**. Despite the presence of a single chelating $[AlCl_4]^-$ anion, the geometry and bond distances about mercury in compound **5** are similar to those in $[Hg(C_6H_5R)_2(MCl_4)_2]$ (see Table 1). A weak interaction (along the crystallographic *a*-axis) between the cation and anion in adjacent chains (Hg···Cl = 3.29 Å) is close to the sum of the van der Waal radii, and the geometry about the mercury is distorted due to this weak interaction, see Figure 6.

A consideration of the orientation of the MCl_3 unit (Figures 2, 3, and 5) shows that the longer terminal M−Cl is oriented toward the mercury. The resulting Hg···Cl distances (3.56−3.83 Å) are outside what would ordinarily be considered a bonding interaction; however, the effect on the M−Cl distance and the orientation of the MCl_3 unit suggest that there is an electrostatic interaction between the chloride and the mercury. While this long-range interaction is symmetrical in compounds **1**−**4** due to their C_2 axis symmetry, a distinct asymmetry is observed for compound **7** [Hg(1)···Cl(11) = 3.57 Å, Hg(1)···Cl(23) = 3.68 Å]. Upon a comparison of the Hg···Cl−Al interactions in compounds **1**, **7**, and **5** we can propose that these structures are part of a continuum between neutral (covalent) and ionic structures (Scheme 1). This observation offers the question: *is the interconversion of neutral and ionic structures facile?*

NMR and UV−Visible Spectroscopy. As noted above we are unable to obtain solution ^1H and ^{13}C NMR spectra for compounds **1**−**8** due to a facile H/D exchange. Dissolution of compounds **1**−**8** in C_6D_6 results in H/D exchange and the formation of C_6D_5H and the appropriate substituted arene, that is, $C_6D_{6-x}Me_x$.[26] Unfortunately, $Hg(arene)_2(MCl_4)_2$ compounds are insoluble in fluorinated solvents (i.e., Freon), and adverse reactions occur in CS_2 or chlorinated solvents.

Solid-state ^{13}C CPMAS NMR spectra have been obtained for compounds **1**−**8**, see Experimental Section. Peak assignments were obtained by a combination of dipolar dephasing experiments[27] and comparison with calculated (DFT) chemical shifts (see Experimental Section). Table 2 gives a comparative example of the calculated and experimental ^{13}C NMR shifts for compounds **1** and **5**. It is interesting to note that the number of aromatic/aliphatic resonances correlates well with the crystallographic symmetry. For example, the toluene molecules in compound **1** are related by crystallographic C_2 symmetry, and the ^{13}C CPMAS NMR spectrum shows a single $\underline{C}H_3$ resonance and four $\underline{C}H$ resonances (one of which is due to two overlapping resonances). In contrast, the ^{13}C CPMAS NMR spectrum for compound **7** shows two sets of resonances for magnetically distinct C_6H_3-1,2,3-Me_3 ligands (see Figure 7a) consistent with the two crystallographically independent ligands per mercury center (see Figure 5). A dipolar dephasing experiment was performed (total dephasing delay = 50 ms) to identify the methyl-substituted aromatic carbon signals. In the case of compound **7**, six of the original aromatic resonances are suppressed as a result of the dipolar dephasing experiment (see Figure 7b).

A common observation for the ^{13}C CPMAS spectra of compounds **1**−**6** is that all but one of the aromatic C−H signals are unusually deshielded and the other is exceptionally shielded (δ 100−106 ppm). A similar shielding effect was observed for

Scheme 1. Schematic Representation of the Potential Interconversion from Neutral $[Hg(arene)_2(AlCl_4)_2]$ (cf, **1** and **3**) to Cationic $[Hg(arene)_2(AlCl_4)_2]^+$ (cf., **5**) via an Asymmetrical Complex (cf, **7**)

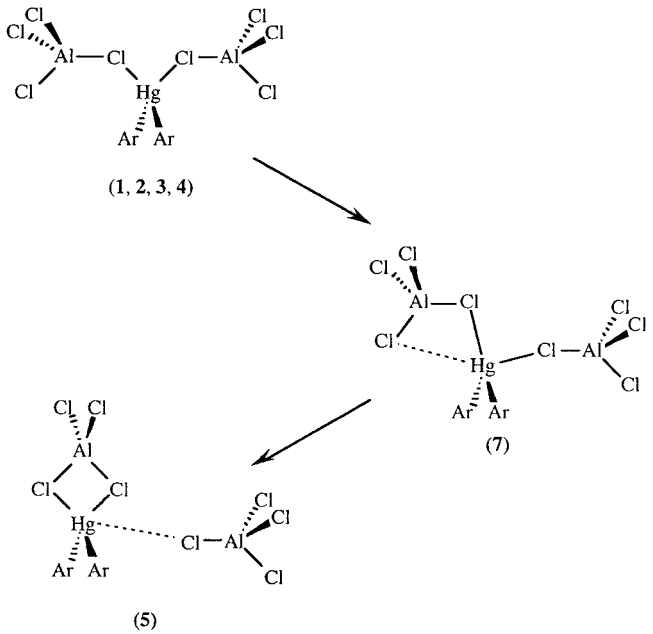

Table 2. Experimental and Calculated (DFT) ^{13}C NMR Spectra

compound	atom[a]	calcd shift δ (ppm)	exptl shift δ (ppm)
$Hg(C_6H_5Me)_2(AlCl_4)_2$	C(1)	155.7	159.4
(**1**)	C(2)	132.5	136.6
	C(3)	135.6	140.1
	C(4)	104.1	100.7
	C(5)	138.0	143.1
	C(6)	132.4	136.6
	C(11)	25.5	24.0
$[Hg(C_6H_4Me_2)_2(AlCl_4)]^+$	C(11)	156.8	158.4
(**5**)	C(12)	146.7	147.7
	C(13)	138.9	139.0
	C(14)	102.4	105.5
	C(15)	130.3	135.6
	C(16)	134.1	139.0
	C(111)	24.7	22.4
	C(112)	23.5	22.4

[a] See Figures 2 and 4 for atom numbering scheme.

(26) This exchange reaction is explored in detail elsewhere.

(27) Alemany, L. B.; Grant, D. M.; Alger, T. D.; Pugmire, R. J. *J. Am. Chem. Soc.*, **1983**, *105*, 6697.

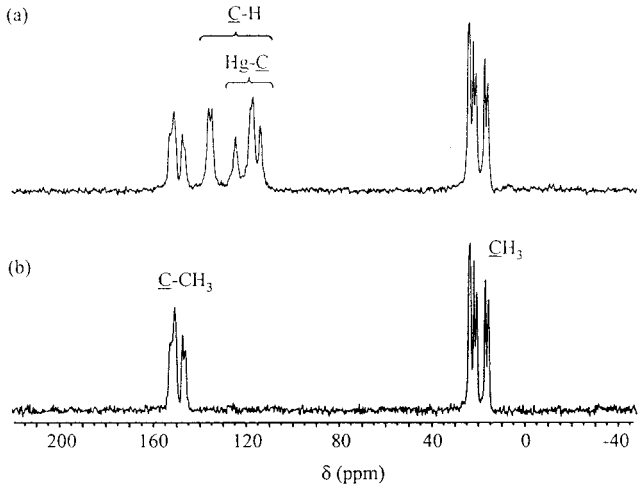

Figure 7. ^{13}C CPMAS NMR spectra of $Hg(C_6H_3\text{-}1,2,3\text{-}Me_3)_2(AlCl_4)_2$ (**7**) showing the presence of magnetically inequivalent arene ligands (a). The identity of the methyl-substituted aromatic carbon signals is enabled by a dipolar dephasing experiment (b) in which the aromatic CH resonances are suppressed.

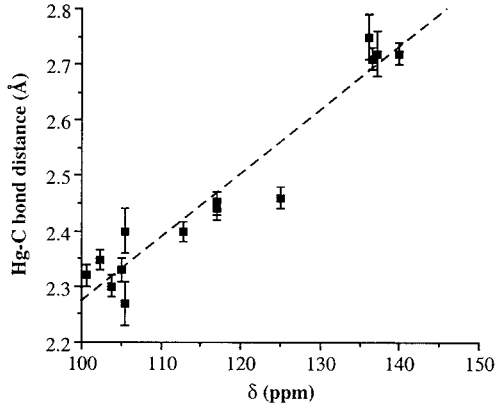

Figure 8. Plot of the crystallographic Hg−C bond distance (with esd's) versus the ^{13}C CPMAS NMR chemical shift for the aromatic carbons with the closest Hg···C contacts in $Hg(arene)_2(MCl_4)_2$.

the C_6HMe_5 and 1,2,4,5-$C_6H_2Me_4$ complexes of $Hg(SbF_6)_2$.[15b] Unfortunately, no detectable $J(^{199}Hg-^{13}C)$ multiplets are evident that might help identify the signals of the carbons coordinated to the mercury. However, based on DFT calculations (Table 2), the most shielded aromatic C−H signal in each spectrum can be assigned to the carbon bound to mercury. The presence of a single Hg−C resonance for compounds **1**−**6** is consistent with η^1 rather than η^2 coordination of the arene. In contrast, the ^{13}C CPMAS spectra of compounds **7** and **8** show four resonances associated with Hg···C interactions (e.g., see Figure 7a). These resonances are in the range 112−125 ppm, significantly removed from the range observed for compounds **1**−**6**. This difference may be rationalized by a consideration of the relative Hg···C distances in the X-ray structure of compound **7** in comparison to those in compounds **1**−**5**. Figure 8 shows a plot of Hg···C distance versus the ^{13}C CPMAS chemical shifts for the two closest arene carbon atoms in compounds **1**−**5** and **7**. Clearly, a correlation between Hg···C distance versus the ^{13}C chemical shift exists. Three observations may be made from the data in Figure 8. First, compounds **1**−**5** are indeed best considered to have η^1 coordination of the arene in the solid state, whereas coordination in compound **7** is best described as η^2. Second, given the similarity of the ^{13}C CPMAS NMR chemical shift for compounds **5** and **6**, as well as compounds **7** and **8**, the solid-state structures of the gallium analogues of compounds **5** and **7** may be predicted to be isostructural. Third, ^{13}C CPMAS NMR may be used as a structural probe for these complexes.

Table 3. UV−Visible Spectra of $Hg(arene)_2(MCl_4)_2$[a]

M	arene	λ (nm)	ε ($mol^{-1}cm^{-1}$)	notes
Al	C_6H_6	285	2000	*b*
Al	C_6H_5Me	325	4500	
Al	C_6H_5Et	288	1300	*c*
		297	1300	
Al	*o*-$C_6H_4Me_2$	337	4300	
Al	*m*-$C_6H_4Me_2$	331	6500	*b*
Al	*p*-$C_6H_4Me_2$	310	7000	*b*
Al	C_6H_3−1,2,3-Me_3	301	2500	*c*
		315	2000	
Ga	C_6H_6	279	5000	*b*
Ga	C_6H_5Me	305	7000	
Ga	C_6H_5Et	289	5300	*c*
		298	5600	
Ga	*o*-$C_6H_4Me_2$	334	6500	
Ga	*p*-$C_6H_4Me_2$	332	4000	*b*
Ga	C_6H_3−1,2,3-Me_3	301	2400	*c*
		320	2300	

[a] $[Hg(O_2CCF_3)_4(C_6H_{6-n})Me_n)_2]$, $\lambda = 288-315$ nm. [b] Upper layer of liquid clathrate, see text. [c] Two well resolved peaks.

We have been unable to obtain satisfactory ^{199}Hg solution NMR for any of the compounds and we were able to obtain a solid-state ^{199}Hg MAS NMR (35.84 MHz) spectra only for $Hg(C_6H_5Me)_2(GaCl_4)_2$ (**2**).[17] However, it is interesting that the observed chemical shift (δ −1970) is downfield from that reported for $HgCl_2$ (δ −1497 ppm)[28] and closer to that of Hg^{2+} aqueous salts (δ −2253 to −2361 ppm)[29] than simple Lewis base complexes, for example, $[HgCl_2\{P(^nBu)_3\}_2]$ (δ −404 ppm).[30] Thus, ^{199}Hg NMR spectroscopy is consistent with a highly electropositive mercury center.[31]

The solid-state ^{27}Al MAS NMR spectrum of compound **5** shows a single resonance with two maxima,[32] while the solution ^{27}Al NMR spectrum shows a single complex resonance at 105 ppm. Similar complex spectra are observed for compounds **1** and **7**, see Experimental Section. The chemical shifts of the ^{27}Al NMR resonances are similar to those previously reported for the $[AlCl_4]^-$ anion.[30]

The UV−visible spectra of compounds **1**−**8** (as well as those of the upper layer of the liquid clathrates described below) are given in Table 3. It is interesting to note that the UV−visible spectrum of compound **5** follows the trend for compounds **1**, **3**, and **7**, suggesting that in solution, compound **5** exists as a neutral complex in *o*-xylene solution. Compounds **3**, **4**, **7**, and **8** all show two well-resolved peaks with similar molar absorptivities; however, it is unclear whether this is due to the lowering of symmetry or the presence of two isomers in solution. A comparison of the UV−visible spectra for the gallium compounds with their aluminum analogues shows that the absorptions are generally similar. On the basis of DFT calculations the UV−visible absorption is found to be due to an $arene_\pi \rightarrow Hg_s$ charge transfer, see below.

(28) Sens, M. A.; Wilson, N. K.; Ellis, P. D.; Odom, J. D. *J. Magn. Reson.* **1974**, *15*, 191.
(29) (a) Maciel, G. E.; Borzo, M. *J. Magn. Reson.* **1973**, *10*, 388. (b) Krüger, H.; Lutz, O.; Nolle, A.; Schwenk, A. *Z. Physik.* **1975**, *A273*, 325.
(30) Kidd, R. G.; Goodfellow, R. J. In *NMR and the Periodic Table*; Harris, R. K., Mann, B. E., Eds.; Academic Press: New York, 1978; Chapter 8, p 195.
(31) Petrosyan, V. S.; Reutov, O. A. *J. Organomet. Chem.* **1974**, 76, 123.
(32) (a) Alemany, L. B. *Appl. Magn. Reson.* **1993**, *4*, 179. (b) Smith, M. E.; van Eck, E. R. H. *Prog. Nucl. Magn. Reson. Spectrosc.* **1999**, *34*, 159.

Table 4. Calculated Bond Lengths (Å) and Angles (deg) in $Hg(arene)_2(MCl_4)_2$ and $[Hg(arene)_2(AlCl_4)]^+$

	$Hg(arene)_2(MCl_4)_2$			$[Hg(arene)_2(AlCl_4)]^+$			
	calcd		exptl	calcd			exptl
	C_6H_6	C_6H_5Me		C_6H_6	C_6H_5Me	*o*-$C_6H_4Me_2$	
Hg−C	2.402	2.382	2.32(1)	2.371	2.349	2.496, 2.561	2.27(2), 2.40(2)
Hg···C	2.900	2.863	2.72(1)	2.782	2.812	2.351	2.64(2), 2.74(2)
Hg−Cl	2.463	2.471	2.677(2)	2.466	2.554	2.741	2.761(3), 2.768(3)
$Al-Cl_{br}$	2.393	2.383	2.176(4)	2.364	2.353	2.349, 2.365	2.166(4), 2.156(5)
$Al-Cl_{ter}$	2.200−2.245	2.204−2.243	2.102(5)−2.118(3)	2.181	2.184	2.186	2.09(1)−2.169(5)
Cl−Hg−Cl	95.94	102.20	81.1(1)	85.24	84.61	83.58	75.2(1)
C−Hg−C	109.37	112.51	135.1(5)	110.06	111.75	108.99	125.5(6)
Hg−Cl-M	119.43	117.85	110.2(2)	92.49	91.32	91.93, 93.21	90.8(1), 91.2(1)

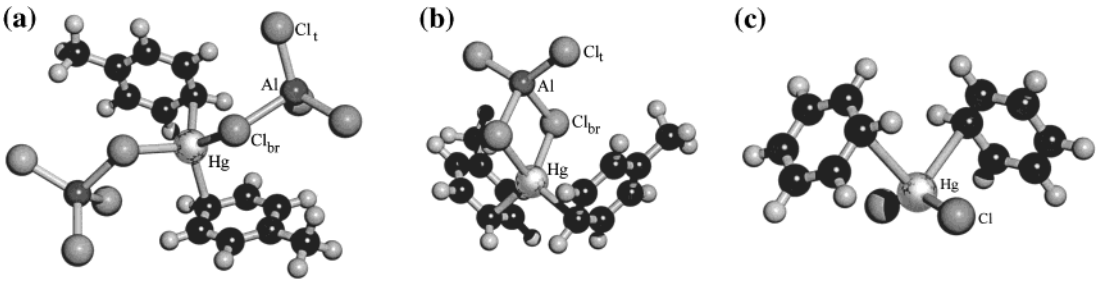

Figure 9. Calculated structures for (a) $Hg(C_6H_5Me)_2(AlCl_4)_2$, (b) $[Hg(C_6H_5Me)_2(AlCl_4)]^+$ and (c) $Hg(C_6H_6)_2Cl_2$.

The absorptions for $Hg(arene)_2(AlCl_4)_2$ are all at higher energies compared to their gallium analogues, suggesting a stronger Hg···arene interaction in the former, in line with expected differences in Lewis acidity between $GaCl_3$ and $AlCl_3$. Finally, it should be noted, that while the absorption for $[Hg_2(\mu\text{-}O_2CCF_3)_4(arene)_2]$ is transient,[12,13] the absorptions for $Hg(arene)_2(MCl_4)_2$ are sustained indefinitely.

DFT Calculations. To better understand the relationship between the neutral and ionic structures as well as to assign the ^{13}C NMR spectra, DFT calculations were performed at the B3LYP level using the 6-31G** basis set for C and H and Stuttgart RLC ECP basis set for Hg, Cl and Al. Calculations were performed on $Hg(C_6H_6)_2(AlCl_4)_2$, $Hg(C_6H_5Me)_2(AlCl_4)_2$, $[Hg(C_6H_6)_2(AlCl_4)]^+$, $[Hg(C_6H_5Me)_2(AlCl_4)]^+$, and $[Hg(o\text{-}C_6H_4Me_2)_2(AlCl_4)]^+$. The optimized calculated structural parameters for each model compound are given in Table 4 along with the appropriate crystallographic data. Exemplary calculated structures for $Hg(C_6H_5Me)_2(AlCl_4)_2$ and $[Hg(C_6H_5Me)_2(AlCl_4)]^+$ are shown in Figure 9a and b, respectively.

The calculated structures of $Hg(arene)_2(AlCl_4)_2$ correspond to a true energy minimum, having all positive vibrational frequencies. In contrast, in the case of $[Hg(o\text{-}C_6H_5Me)_2(AlCl_4)]^+$ one imaginary frequency was calculated for the minimized structure indicating a first-order saddle point. The 3D potential energy surface of $[Hg(o\text{-}C_6H_4Me_2)_2(AlCl_4)]^+$ is very shallow, for example, the energy difference between C_s and C_1 symmetries is only 0.71 kJ·mol^{-1}.

As may be seen from Table 4, the overall structures for both neutral and cationic structures are reasonably reproduced at the present level of theory. However, the Hg−C distances are calculated to be slightly longer than those observed in the crystal structures, while the Hg−Cl distances are underestimated. Despite these differences, the calculated ^{13}C NMR shifts are very close to those observed in the solid-state ^{13}C CPMAS NMR, see Table 2.

The Hg···arene interaction is best described as being strongly ionic in character with small contributions from the s and p orbitals on mercury. In addition, there appears to be no d character in the bonding. As may be seen from Figure 10, the bonding orbital surfaces for $Hg(C_6H_5Me)_2(AlCl_4)_2$ have a strong delocalized component across the $AlCl_3$ units. It is clear from the DFT calculations that the Hg···arene interaction involves two π orbitals on each arene (**I** and **II**). Such a combination agrees with the asymmetric bonding of the arene to mercury, see above.

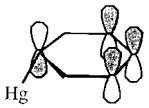

(**I**)

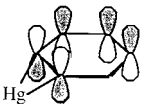

(**II**)

On the basis of the calculated energy [339 kJ·mol^{-1} (C_6H_6) and 330 kJ·mol^{-1} (C_6H_5Me)] for the dissociation of one $[AlCl_4]^-$ group from $Hg(arene)_2(AlCl_4)_2$ (eq 3), the cation−anion interaction is clearly very strong.

$$Hg(arene)_2(AlCl_4)_2 \rightarrow [Hg(arene)_2(AlCl_4)]^+ + [AlCl_4]^- \quad (3)$$

It is interesting that the dissociation of $AlCl_3$ from $Hg(C_6H_6)_2(AlCl_4)_2$ (eq 4) is more favored (112 kJ·mol^{-1}) than the dissociation of $[AlCl_4]^-$ (eq 3).

$$Hg(C_6H_6)_2(AlCl_4)_2 \rightarrow HgCl(C_6H_6)_2(AlCl_4) + AlCl_3 \quad (4)$$

We have no evidence for the dissociation of $AlCl_3$ (or $GaCl_3$) in solution, suggesting that the formation in the solid state of the ionic structure (i.e., the *o*-xylene derivatives) is due to a large lattice stabilization energy. Furthermore, the formation of ionic species in solution (see below) must be moderated by strong ion solvation.

As noted above, the UV−visible spectra of compounds **1**−**8** consist of an absorption for $Hg(arene)_2(MCl_4)_2$ and are all between 279 and 337 nm, resulting in a characteristic yellow to orange color. Single-excitation configuration interaction (CIS) calculations were performed on the neutral complexes $Hg(C_6H_6)_2(AlCl_4)_2$, $Hg(C_6H_5Me)_2(AlCl_4)_2$, and $[Hg(o\text{-}C_6H_4Me_2)_2(AlCl_4)]^+$. Three singlet excited states were calculated for each of the complexes. Although the calculated excitation energies are about 6−17% higher than the experimentally determined

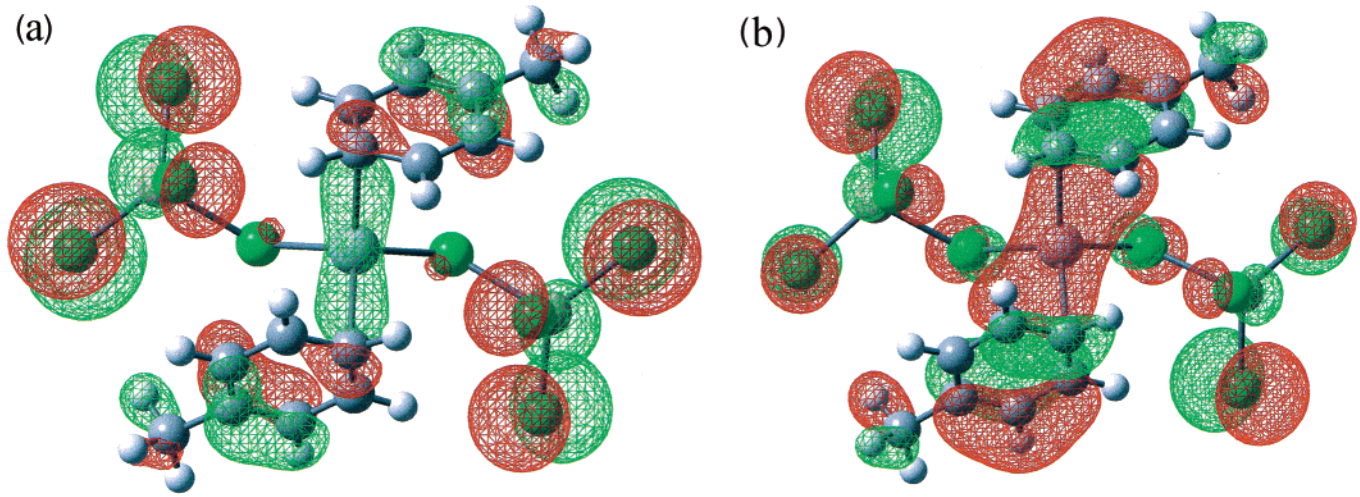

Figure 10. Calculated surfaces for the Hg···arene interaction in $Hg(C_6H_5Me)_2(AlCl_4)_2$.

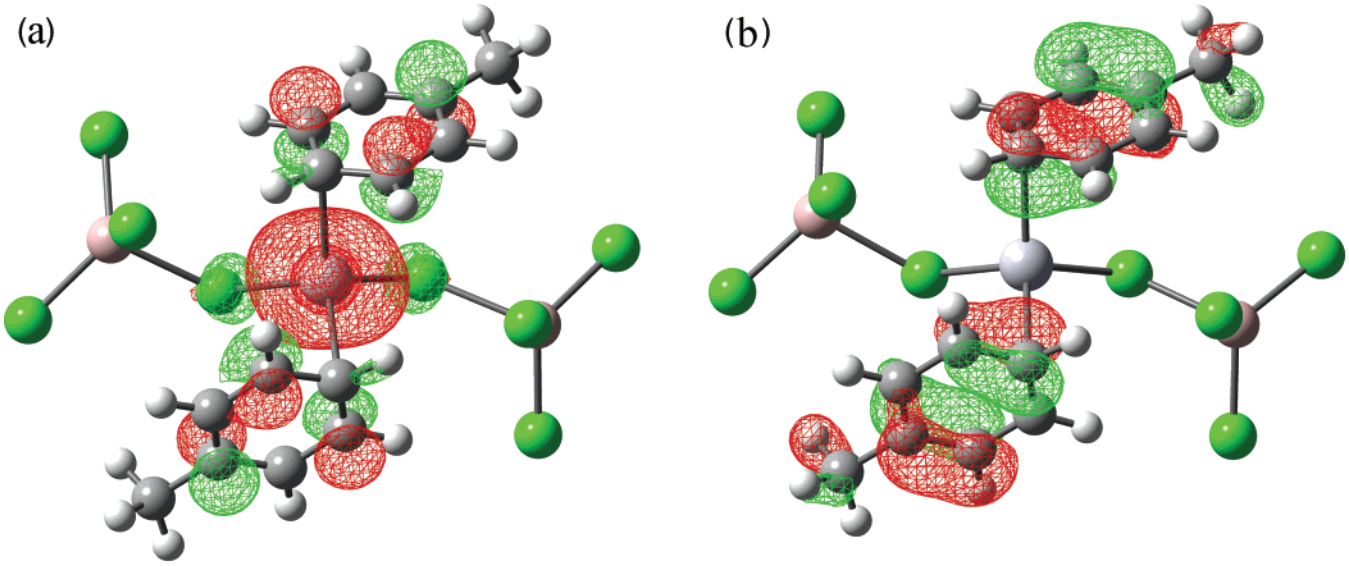

Figure 11. Calculated LUMO (a) and HOMO (b) surfaces of $Hg(C_6H_5Me)_2(AlCl_4)_2$.

values,[33] their trend is undoubtedly correct. All of the calculated excited states have similar excitation energies, and each occurs between the HOMO (or a filled molecular orbital close in energy) and the LUMO. As may be seen from Figure 11b, the HOMO surface for $Hg(C_6H_5Me)_2(AlCl_4)_2$ is essentially a combination of aromatic π orbitals. The other two energetically similar filled orbitals are also aromatic π in character. The major contribution of the LUMO (Figure 11a) comes from the Hg 6s orbital. Thus, the observed UV−visible spectra are due to an $\text{arene}_\pi \rightarrow \text{Hg}_s$ charge transfer.

Liquid Clathrates. As noted above, the reaction of $HgCl_2$ with MCl_3 in benzene, *m*-$C_6H_4Me_2$, *p*-$C_6H_4Me_2$ yields liquid clathrates, for example, Figure 12. Clathrate formation is concentration-dependent. Thus, if $HgCl_2$ and $AlCl_3$ are reacted in benzene at a concentration below 0.01 M (Hg) a homogeneous solution is formed; above this threshold value, the clathrate forms. The threshold for *m*-$C_6H_4Me_2$ and *p*-$C_6H_4Me_2$ is 0.16 and 0.05 M, respectively.

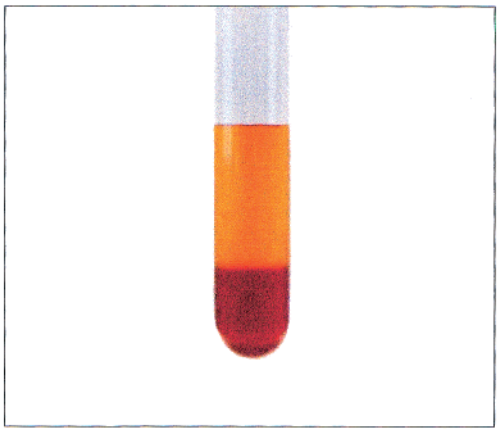

Figure 12. Liquid chlathrate formed from the reaction of $HgCl_2$ with $AlCl_3$ in *p*-xylene showing the presence of two colored layers associated with neutral (upper) and ionic (lower) complexes.

The upper layer of the clathrate in each case is pale yellow in color, while the lower layers are bright orange, see Figure 12. The layers can be separated by decanting the upper layer. The homogeneous solutions formed below the threshold con-

(33) The overstimation of excitation energies has been previously reported for a number of simple molecules, see: (a) Foresman, J. B.; Frisch, A. E. *Exploring Chemistry with Electronic Structue Methods*, 2nd ed.; Gaussian: Pittsburgh, PA, 1996; Chapter 9. (b) Muguruma, C.; Koga, N.; Hatanaka, Y.; El-Sayed, I.; Mikami, M.; Tanaka, M. *J. Phys. Chem.* **2000**, *104*, 4928.

centrations are spectroscopically identical to the upper layer of the clathrate. Conductivity measurements on the individual layers indicate that the species in the upper layer are neutral, while those in the lower layer are 1:1 electrolytes. The arene:Hg ratio of the clathrates was determined to be ca. 8.5 for C_6H_6 and *m*-$C_6H_4Me_2$, and ca. 7.5 for *p*-$C_6H_4Me_2$. The formation of the clathrates is summarized by the equilibrium in eq 5.

$$Hg(arene)_2(AlCl_4)_2 + n\ arene \rightleftharpoons [Hg(arene)_2(AlCl_4)][AlCl_4]\cdot n(arene) \quad (5)$$

The concentrations of the upper layer of the benzene and *p*-xylene clathrates are insufficient to allow for NMR characterization. In contrast, the *m*-xylene clathrate exhibits a ^{27}Al NMR spectrum identical to that observed for the isolable neutral compounds. The concentrations of the upper layer for all the clathrates (and the homogeneous solutions) are suitable for UV visible spectroscopy and are shown in Table 2. In each case, the spectra are similar to those of the isolated compounds, Hg(arene)$_2$(MCl$_4$)$_2$.

The ^{27}Al NMR spectra of the lower clathrate layers show single broad resonances consistent with $AlCl_4^-$. The ^{13}C NMR spectra of the clathrates shows a single set of resonances for the arene, suggesting that there is a dynamic equilibria between coordinated and "free" arene. The ^1H NMR the C$\underline{H}_3$ resonances (for *m*- and *p*-xylene) appear as a single sharp signal, but the aromatic $\underline{C}$H signals are very broad, suggesting a second slower exchange process. This may be accounted for by a degenerate H/H exchange of the aromatic CH groups, related to the H/D exchange observed in deuterated solvents.

The term "liquid clathrates" is generally used to designate nonstoichiometric liquid inclusion compounds which form upon the interaction of aromatic molecules with certain ionic moieties.[34] It is generally believed that liquid clathrates are formed when the parent compound possesses the following conditions: the substance must have a relatively low lattice energy; the substance must be capable of exhibiting a very strong cation−anion interaction; association into tight ion pairs or other units must be prevented. The lattice energy for Hg(arene)$_2$(MCl$_4$)$_2$ should be low, given the lack of any unusual intermolecular distances in the solid state, and thus meets the first requirement. Based upon the calculated energy (ca. 330 kJ·mol^{-1}) for the dissociation of one $AlCl_4^-$ group from Hg(arene)$_2$(AlCl$_4$)$_2$ (eq 3), the cation−anion interaction is clearly strong. From conductivity measurements which confirm a 1:1 electrolyte, we may presume that the aromatic molecules strongly solvate the ions precluding ion pair formation.

We note that the clathrates reported herein are distinct from the more usual class of clathrates. In a traditional clathrate the upper layer is essentially solvent, while the lower "clathrate" layer contains the ionic salts and solvent. In our clathrates, the upper layer contains a neutral component "Hg(arene)$_2$(MCl$_4$)$_2$", while the lower contains the ionic component "[Hg(arene)$_2$(MCl$_4$)][MCl$_4$]". The presence of mercury arene complexes in both layers is clearly seen in the photograph shown in Figure 12.

Activation of $HgCl_2$ toward Arene Binding by MCl_3. As noted in the Introduction, Hg···arene complexes have been characterized spectroscopically.[15] Unfortunately, the Hg···arene interaction in $HgCl_2$(arene)$_2$ is not sufficiently robust to allow for crystallization and X-ray structural characterization. A measure of the effectiveness of MCl_3 in increasing the Lewis acidity of the mercury, and thus enhancing the coordination of arenes, may be obtained from (a) UV−visible spectroscopy and (b) DFT calculations.

The UV spectrum of $HgCl_2$ dissolved in toluene has been reported to consist of an absorption at 274 nm.[15] The spectral bands observed for compounds **1** (325 nm) and **2** (305 nm) are at a lower energy than that of the $HgCl_2$ complex, indicative of a greater decrease in the $\pi-\pi^*$ energy in the arene ring for the mixed metal complexes.

DFT calculations were performed on Hg(C$_6$H$_6$)$_2$Cl$_2$ at the B3LYP level using the 6-31G** basis set for C and H and Stuttgart RLC ECP basis set for Hg and Cl; the calculated structure is shown in Figure 9c. The Hg−Cl distances in Hg(C$_6$H$_6$)$_2$Cl$_2$ (2.311 Å) are significantly shorter than in the calculated structure of Hg(C$_6$H$_6$)$_2$(AlCl$_4$)$_2$ (2.463 Å) and approach the values observed in $HgCl_2$ by X-ray crystallography [2.283(9) Å].[35] This is expected in comparing a terminal versus bridging chloride ligand. Also, the Cl−Hg−Cl angle calculated for Hg(C$_6$H$_6$)$_2$Cl$_2$ (152.3°) is closer to linear (as in $HgCl_2$) than the equivalent angles in Hg(arene)$_2$(AlCl$_4$)$_2$ [experimental = 75.2(1)−89.90(8)°, calculated = 95.94−102.20°]. More importantly, the closest Hg···C interactions in Hg(C$_6$H$_6$)$_2$Cl$_2$ (2.813 Å) are significantly larger than those calculated for Hg(C$_6$H$_6$)$_2$(AlCl$_4$)$_2$ (2.402 Å). Thus, the presence of $AlCl_3$ decreases the Hg···C distance by ca. 0.4 Å; a significant activation. Furthermore, it is worth noting that the Hg···C interaction in Hg(C$_6$H$_6$)$_2$Cl$_2$ is comparable to the second closest distance in Hg(C$_6$H$_6$)$_2$(AlCl$_4$)$_2$, which, based upon ^{13}C spectroscopy, is very weak.

Conclusions

We have demonstrated that group 13 Lewis acids may be used to "activate" other Lewis acidic complexes. In this regard, stable Hg···arene complexes have been prepared by the reaction of $HgCl_2$ with 2 mol equiv of MCl_3 (M = Al, Ga) in an aromatic solvent.[36] For C_6H_5Me, C_6H_5Et, *o*-$C_6H_4Me_2$, and C_6H_3-1,2,3-Me_3 a neutral complex Hg(arene)$_2$(MCl$_4$)$_2$ is formed in solution and retained in the solid state except with *o*-$C_6H_4Me_2$, for which an ionic structure is observed. In contrast, reaction of $HgCl_2$ with MCl_3 in benzene, *m*-$C_6H_4Me_2$, *p*-$C_6H_4Me_2$ yields liquid clathrates. We propose that the upper layer of each clathrate contains a dilute solution of the neutral compound, Hg(arene)$_2$(MCl$_4$)$_2$, while the lower layer is consistent with a 1:1 electrolyte system, that is, [Hg(arene)$_2$(MCl$_4$)][MCl$_4$]. On the basis of the high calculated energy for dissociation of $[AlCl_4]^-$ from the neutral complex we propose that the formation of ionic compounds is energetically moderated by the formation of the clathrates. It is unclear at this time what factors control the formation of a neutral complex versus a clathrate, and why only the *o*-$C_6H_4Me_2$ derivative exists as a cation/anion pair in the solid state. We are continuing our studies on these mercury−arene complexes, in particular, their application as H/D exchange catalysts.

The Hg···arene interaction in Hg(arene)$_2$(MCl$_4$)$_2$ and Hg(arene)$_2$(MCl$_4$)][MCl$_4$] is significantly stronger than for either of the constituent halides, that is, $HgCl_2$ or MCl_3. Thus, the group 13 halides appear to activate the mercury toward the

(34) (a) Atwood, J. L.; Atwood, J. D. In *Inorganic Compounds with Unusual Properties*; King, R. B., Ed.; Advances in Chemistry, Vol. 150; American Chemical Society, Washington, DC, 1976; Chapter 11. (b) Atwood, J. L. In *Recent Developments in Separation Science*; Li, N. N., Ed.; CRC Press: Cleveland, 1977; Vol. 3, pp 195−209. (c) Atwood, J. L. In *Inclusion Compounds*; Atwood, J. L., Davies, J. E. D., MacNicol, D. D., Eds.; Academic Press: London, 1984; Vol. 1, pp 375−405.

(35) Subramanian, V.; Seff, K. *Acta Crystallogr.* **1980**, *B36*, 2132.

(36) We note that stable silver arene complexes have been prepared by the Lewis acid abstraction of fluoride from AgF, see: Hatop, H.; Roesky, H. W.; Labahn, T.; Roepken, C.; Sheldrick, G. M.; Bhattacharjee, M. *Organometallics* **1998**, *17*, 4326.

coordination of the arenes. Based upon X-ray crystallography, ^{13}C CPMAS NMR spectroscopy, and DFT calculations the Hg···arene interaction is found to range from predominantly η^1 coordination to close to η^2 coordination. At this time we are unclear as to the factors that control the mode of coordination.

Experimental Section

NMR spectra were obtained on Bruker AM-250 and Avance 200, 400, and 500 spectrometers. Chemical shifts are reported relative to internal solvent resonances. ^{13}C and ^{199}Hg MAS spectra were obtained at 50.32 and 35.84 MHz respectively, using Bruker Avance 200 spectrometer. A 7 mm zirconium dioxide rotor was used for all spectra, with the spin rates up to 7 kHz. ^{199}Hg spectra were recorded with direct polarization (4 μs 28° rf pulses). Centerband signals were located by varying the spinning rate. A 20.53 ms FID was acquired with high level proton decoupling and a 50 s relaxation delay without decoupling. A total of 1024 scans were required to get acceptable spectra. The FID was processed with 70 Hz of line broadening. Chemical shift was referenced using 0.5 M solution of $HgCl_2$ in 75% EtOH with 25% of D_2O ($\delta_{Hg} = -1497$ ppm).[37] Mass spectra were obtained on a Finnigan MAT 95 mass spectrometer operating with an electron beam energy of 70 eV for EI mass spectra. UV−visible spectral data were recorded on a Varian Cary 4 spectrometer and are given in Table 3. Microanalyses were performed by Oneida Research Services, Inc., Whitesboro, NY. Unfortunately, the extreme air sensitivity of several compounds resulted in highly variable analysis results. The synthesis of $Hg(C_6H_5Me)_2(GaCl_4)_2$ (**2**) was reported previously.[17] Solvents and all arenes were distilled and degassed prior to use.

$Hg(C_6H_5Me)_2(AlCl_4)_2$ (1). Toluene (25 mL) was added to the solid mixture of anhydrous $HgCl_2$ (1.00 g, 3.68 mmol), and $AlCl_3$ (0.984 g, 7.37 mmol). The resulting yellow solution was heated at approximately 100 °C while being vigorously stirred to allow all $HgCl_2$ to dissolve. In about 15 min, heating was stopped, and the reaction flask was wrapped in aluminum foil to prevent the decomposition reaction caused by bright light. Yellow crystals grew within 1 h at room temperature. Yield: 90%. Mp 95 °C. ^{13}C CPMAS NMR (50.32 MHz): δ 159.4 (1C, C*Me), 143.1 (1C, *m*-CH), 140.1 (1C, *m*-CH), 136.6 (2C, *o*-CH), 100.7 (1C, Hg···CH), 24.0 (1C, CH_3). ^{27}Al NMR (52.15 MHz, toluene with C_6D_6 as an external reference): δ 105 ($W_{1/2} = 780$ Hz). ^{27}Al MAS NMR (52.15 MHz): δ 118 and 86 ($W_{1/2} = 3370$ Hz).[32]

$Hg(C_6H_5Et)_2(AlCl_4)_2$ (3). Prepared in a manner similar to that for compound **1**, but using ethylbenzene (25 mL), anhydrous $HgCl_2$ (1.00 g, 3.68 mmol), and $AlCl_3$ (0.984 g, 7.37 mmol) to yield yellow crystals. Yield: 80%. Mp 74 °C. ^{13}C CPMAS NMR (50.32 MHz): δ 163.2 (1C, CCH_2), 140.2 (1C, *m*-CH), 137.1 (1C, *m*-CH), 135.9 (*o*-CH), 103.7, (1C, Hg···CH), 30.8 (1C, CH_2), 15.4 (1C, CH_3).

$Hg(C_6H_5Et)_2(GaCl_4)_2$ (4). Prepared in a manner similar to that for compound **1**, but using ethylbenzene (25 mL), anhydrous $HgCl_2$ (1 g, 3.68 mmol), and $GaCl_3$ (1.298 g, 7.37 mmol). Yellow crystals were grown within 1 h at room temperature. Yield: 78%. Mp 59 °C. ^{13}C CPMAS NMR (50.32 MHz): δ 162.8 (1C, CCH_2), 139.9 (1C, *m*-CH), 136.2 (3C, *m*-CH and *o*-CH), 105.0 (1C, Hg···CH), 30.9 (1C, CH_2), 16.2 (1C, CH_3).

$[Hg(o\text{-}C_6H_4Me_2)_2(AlCl_4)][AlCl_4]$ (5). Prepared in a manner similar to that for compound **1**, but using *o*-xylene (25 mL), anhydrous $HgCl_2$ (1.00 g, 3.68 mmol), and $AlCl_3$ (0.984 g, 7.37 mmol) to yield dark-yellow crystals. Yield: 80%. Mp 99 °C. ^{13}C CPMAS NMR (50.32 MHz): δ 158.4 (1C, CCH_3), 147.7 (1C, CCH_3), 139.0 (2C, *o*-CH), 135.6 (1C, *m*-CH), 105.5 (1C, Hg···CH), 22.4 (2C, CH_3). ^{27}Al MAS NMR (52.15 MHz): δ 89 and 82 ($W_{1/2} = 870$ Hz). ^{27}Al NMR (52.15 MHz, in *o*-xylene, C_6D_6 as an external lock solvent): δ 105 ($W_{1/2} = 630$ Hz).

$[Hg(o\text{-}C_6H_4Me_2)_2(GaCl_4)][GaCl_4]$ (6). Prepared in a manner similar to that for compound **1**, but using *o*-xylene (25 mL), anhydrous $HgCl_2$ (1.00 g, 3.68 mmol), and $GaCl_3$ (1.298 g, 7.37 mmol), to yield dark-yellow crystals. Yield: 85%. Mp 77 °C. ^{13}C CPMAS NMR (50.32

(37) *NMR and the Periodic Table*; Harris, R. K., Mann, B. E., Eds.; Academic Press: New York 1978; p 268

Table 5. Summary of X-ray Diffraction Data

cmpd	$Hg(C_6H_5Me)_2(AlCl_4)_2$ (**1**)	$Hg(C_6H_5Et)_2(AlCl_4)_2$ (**3**)	$Hg(C_6H_5Et)_2(GaCl_4)_2$ (**4**)	$[Hg(o\text{-}C_6H_4Me_2)_2\text{-}(AlCl_4)][AlCl_4]$ (**5**)	cmpd	$Hg(C_6H_3\text{-}1,2,3\text{-}Me_3)_2(AlCl_4)_2$ (**7**)
empirical formula	$C_{14}H_{16}Al_2Cl_8Hg$	$C_{16}H_{20}Al_2Cl_8Hg$	$C_{16}H_{20}Ga_2Cl_8Hg$	$C_{16}H_{20}Al_2Cl_8Hg$	empirical formula	$C_{18}H_{24}Al_2Cl_8Hg$
M_w	722.42	750.47	835.95	750.47	M_w	778.52
cryst. system	orthorombic	orthorombic	orthorhombic	orthorhombic	cryst. system	monoclinic
space group	*Pbcn*	*Pbcn*	*Pbcn*	$P2_12_12_1$	space group	$P2_1/c$
a, Å	13.428(3)	13.695(3)	13.751(3)	10.309(2)	*a*, Å	14.049(3)
b, Å	12.571(3)	12.671(3)	12.746(3)	13.607(3)	*b*, Å	13.497(3)
c, Å	14.352(3)	15.115(3)	15.065(3)	18.660(4)	*c*, Å	15.469(3)
β, deg					β, deg	103.37(3)
V, Å^3	2422.7(8)	2622.8(9)	2640.5(9)	2617.5(9)	*V*, Å^3	2853(1)
Z	4	4	4	4	*Z*	4
μ, cm^{-1}	1.981	1.901	2.103	1.904	μ, cm^{-1}	1.812
no. collected	5788	6439	4772	11887	no. collected	5924
no. ind	1685	1846	1902	3763	no. ind	3809
no. obsd	1272 ($\|F_o\| > 4.0\sigma\|F_o\|$)	1035 ($\|F_o\| > 4.0\sigma\|F_o\|$)	1243 ($\|F_o\| > 4.0\sigma\|F_o\|$)	2467 ($\|F_o\| > 4.0\sigma\|F_o\|$)	no. obsd	2839 ($\|F_o\| > 4.0\sigma\|F_o\|$)
weighting scheme					weighting scheme	0.0604, 0
SHELXTL parameters	0.123, 0	0.0.0802, 0	0.100, 0	0.1163, 0	SHELXTL parameters	
R	0.0609	0.0609	0.0678	0.0690	*R*	0.0444
R_w	0.1636	0.1449	0.1666	0.1852	R_w	0.1167
largest diff peak, eÅ^{-3}	0.95	1.41	1.96	0.98	largest diff peak, eÅ^{-3}	1.19

MHz): δ 159.0 (1C, $\underline{C}CH_3$), 146.3 (1C, $\underline{C}CH_3$), 139.3 (3C, *o*-$\underline{C}$H and *m*-$\underline{C}$H), 102.9 (1C, Hg···$\underline{C}$H), 22.5 (1C, $\underline{C}H_3$).

$Hg(C_6H_3$-1,2,3-$Me_3)_2(AlCl_4)_2$ (7). Prepared in a manner similar to that for compound **1**, but using 1,2,3-trimethylbenzene (20 mL), anhydrous $HgCl_2$ (0.50 g, 1.84 mmol), and $AlCl_3$ (0.491 g, 3.68 mmol). Yellow crystals were grown over a few days at −19 °C. Yield: 70%. Mp 94 °C. ^{13}C CPMAS NMR (50.32 MHz): δ 153.1 (3C, br, $\underline{C}CH_3$), 148.1 (3C, br, $\underline{C}CH_3$), 136.3 (1C, *o*-$\underline{C}$H), 135.0 (1C, *o*-$\underline{C}$H), 125.1 (1C, Hg···$\underline{C}$H), 117.2 (2C, Hg···$\underline{C}$H), 112.8 (1C, Hg···$\underline{C}$H), 23.8 (2C, $\underline{C}H_3$), 21.6 (1C, $\underline{C}H_3$), 20.4 (1C, $\underline{C}H_3$), 16.9 (1C, $\underline{C}H_3$), 15.5 (1C, $\underline{C}H_3$). ^{27}Al MAS NMR (52.15 MHz): δ 90 and 76 ($W_{1/2}$ = 2040 Hz).[32] ^{27}Al NMR (52.15 MHz, in 1,2,3-trimethylbenzene, C_6D_6 as an external lock solvent): δ 105 ($W_{1/2}$ = 2040 Hz).

$Hg(C_6H_3$-1,2,3-$Me_3)_2(GaCl_4)_2$ (8). Prepared in a manner similar to that for compound **1**, but using 1,2,3-trimethylbenzene (20 mL), anhydrous $HgCl_2$ (0.5 g, 1.84 mmol), and $GaCl_3$ (0.65 g, 3.68 mmol). Yellow crystals were grown over a few days at −19 °C. Yield: 80%. Mp 83 °C. ^{13}C CPMAS NMR (50.32 MHz): δ 152.9 (1C, $\underline{C}CH_3$), 152.2 (1C, $\underline{C}CH_3$), 150.8 (2C, $\underline{C}CH_3$), 147.5 (1C, $\underline{C}CH_3$), 146.4 (1C, $\underline{C}CH_3$), 136.0 (1C, *o*-$\underline{C}$H), 134.7 (1C, *o*-$\underline{C}$H), 124.4 (1C, Hg···$\underline{C}$H), 118.0 (1C, Hg···$\underline{C}$H), 117.0 (1C, Hg···$\underline{C}$H), 113.8 (1C, Hg···$\underline{C}$H), 23.4 (2C, $\underline{C}H_3$), 21.8 (1C, $\underline{C}H_3$), 20.6 (1C, $\underline{C}H_3$), 16.9 (1C, $\underline{C}H_3$), 15.6 (1C, $\underline{C}H_3$).

Liquid Clathrates. To a solid mixture of $HgCl_2$ (1.00 g, 3.68 mmol) and $AlCl_3$ (0.984 g, 7.37 mmol) was added the appropriate arene (10 mL). The resulting yellow-orange solution was stirred vigorously at 60 °C until all of the $HgCl_2$ dissolved. In approximately 30 min stirring was halted, and within a further 5 min the reaction mixture separated into two layers. The bottom chlathrate layer has the general formula, $Hg(arene)_{8.5}(AlCl_4)_2$. Similar chlathrates are observed with $GaCl_3$. UV−visible spectral data are given in Table 3.

C_6H_6. Bottom layer, ^{27}Al NMR (52.15 MHz, C_6D_6 as an external lock solvent): δ 105 ($W_{1/2}$ = 1170 Hz).

***m*-$C_6H_4Me_2$.** Bottom layer, ^{27}Al NMR (52.15 MHz, C_6D_6 as an external lock solvent): δ 104 ($W_{1/2}$ = 1800 Hz). Top layer, ^{27}Al NMR (52.15 MHz, C_6D_6 as an external lock solvent): δ 105 ($W_{1/2}$ = 1210 Hz).

***p*-$C_6H_4Me_2$.** Bottom layer, ^{27}Al NMR (52.15 MHz, C_6D_6 as an external lock solvent): δ 105 ($W_{1/2}$ = 1720 Hz).

Computational Methods. All density functional calculations were carried out using a Gaussian-98 suite.[38] Complete geometry optimizations were performed at B3LYP[39] level using the 6-31G** basis set for C and H and Stuttgart RLC ECP basis set for Hg, Cl, and Al. C_2 and C_s symmetries were imposed on neutral and cationic molecules, respectively. Vibrational frequencies were then evaluated for benzene complexes to verify the existence of the true potential minimum and to determine zero-point energies. ^{13}C NMR chemical shifts for $Hg(C_6H_5Me)_2(AlCl_4)_2$ and $[Hg(o\text{-}C_6H_4Me_2)_2(AlCl_4)]^+$ complexes were calculated at the same level of theory. Vertical excitation energies and corresponding oscillator strengths for $Hg(C_6H_6)_2(AlCl_4)_2$, $Hg(C_6H_5Me)_2(AlCl_4)_2$, and $[Hg(o\text{-}C_6H_4Me_2)_2(AlCl_4)]^+$ were calculated by the single-excitation configuration interaction (CIS)[40] method at the ground-state stationary points of the B3LYP level.

Crystallographic Studies. Data for compounds **1**, **2**−**5**, and **7** were collected on a Bruker CCD SMART system, equipped with graphite monochromated Mo Kα radiation (λ = 0.71073 Å) and corrected for Lorentz and polarization effects. The structures were solved using the direct methods program XS[41] and difference Fourier maps and refined by using full matrix least-squares methods. All non-hydrogen atoms (except the ethyl groups in compounds **3** and **4**) were refined with anisotropic thermal parameters. Hydrogen atoms were introduced in calculated positions and allowed to ride on the attached carbon atoms [d(C−H) = 0.95 Å]. Refinement of positional and anisotropic thermal parameters led to convergence (see Table 5).

Acknowledgment. Financial support for this work is provided by the Robert A. Welch Foundation, including the Bruker CCD Smart System Diffractometer of the Texas Center for Crystallography at Rice University. The Bruker Avance 200 and 500 NMR spectrometers were purchased with funds from ONR Grant N00014-96-1-1146 and NSF Grant CHE-9708978, respectively.

Supporting Information Available: Full listings of bond length and angles, anisotropic thermal parameters, and hydrogen atom parameters; tables of calculated and observed structure factors; optimized structural parameters for DFT calculations; elemental analysis; energies for optimized structures; calculated UV−visible absorption spectra and oscillator strengths (PDF). This material is available free of charge via the Internet at http://pubs.acs.org.

JA011003U

(38) Frisch, M. J.; Trucks, G. W.; Schlegel, H. B.; Scuseria, G. E.; Robb, M. A.; Cheeseman, J. R.; Zakrzewski, V. G.; Montgomery, J. A., Jr.; Stratmann, R. E.; Burant, J. C.; Dapprich, S.; Millam, J. M.; Daniels, A. D.; Kudin, K. N.; Strain, M. C.; Farkas, O.; Tomasi, J.; Barone, V.; Cossi, M.; Cammi, R.; Mennucci, B.; Pomelli, C.; Adamo, C.; Clifford, S.; Ochterski, J.; Petersson, G. A.; Ayala, P. Y.; Cui, Q.; Morokuma, K.; Malick, D. K.; Rabuck, A. D.; Raghavachari, K.; Foresman, J. B.; Cioslowski, J.; Ortiz, J. V.; Baboul, A. G.; Stefanov, B. B.; Liu, G.; Liashenko, A.; Piskorz, P.; Komaromi, I.; Gomperts, R.; Martin, R. L.; Fox, D. J.; Keith, T.; Al-Laham, M. A.; Peng, C. Y.; Nanayakkara, A.; Challacombe, M.; Gill, P. M. W.; Johnson, B.; Chen, W.; Wong, M. W.; Andres, J. L.; Gonzalez, C.; Head-Gordon, M.; Replogle, E. S.; Pople, J. A. *Gaussian 98*, revision A.9; Gaussian, Inc.: Pittsburgh, PA, 1998.

(39) (a) Becke, A. D. *J. Chem. Phys.* **1993**, *98*, 5648. (b) Stephens, P. J.; Devlin, C. F.; Chabalowski, C. F.; Frisch M. J. *J. Phys. Chem.* **1994**, *98*, 11623. (c) Lee, C.; Yang, W.; Parr, R. G. *Phys. Rev.* **1988**, *B37*, 785.

(40) Foresman, J. B.; Head-Gordon, M.; Pople, J. A.; Frisch, M. J. *J. Phys. Chem.* **1992**, *96*, 135.

(41) Sheldrick, G. M. *SHELXTL*; Bruker AXS, Inc.: Madison, Wisconsin, 1997.